Simulation and fabrication of a new phase shifting mask for 0.35 μm contact hole pattern transfer : Halftone-rim

Wen-an Loong, Shyi-long Shy*, Guey-chi Guo and Yueh-lin Chou

Institute of Applied Chemistry, National Chiao Tung University, Hsinchu, Taiwan, Republic of China
*National Nano Device Laboratory, Hsinchu, Taiwan, Republic of China

ABSTRACT

In this paper we report a new type of phase shifting mask (PSM), namely, halftone-rim, which is a combination of rim and halftone. Based on our simulation study using DEPICT-2 simulation tool, the aerial image of halftone-rim PSM in i-line for 0.35 μm contact hole pattern has better contrast and larger total depth of focus (DOF) than other mask techniques, such as conventional, subresolution, rim, and attenuated (halftone). Except attenuated mask, halftone-rim also has higher aerial image intensity among these masks. The preliminary contact hole pattern transfer studies using this new type PSM indicate a resolution down to 0.31 μm and a total DOF of 0.9 μm for contact holes by 5x i-line stepper (NA: 0.5, coherence: 0.6). Further experimental works on optimization of lithographic processes, especially in reactive ion etching of shifter layer and wet etching of halftone chrome, are needed to improve both resolution and total DOF.

1. INTRODUCTION

Phase shifting mask (PSM) could improve both resolution and depth of focus (DOF) without changing much to the exposure system except the lower degree of coherence for stepper. The resolution could reach 0.35~0.40 μm with the combination of PSM technique and conventional i-line (365 nm) process. Different PSMs suit for different circuit patterns because each has its advantages and disadvantages in optical pattern transfer. Rim PSM has the advantage of self-aligned shifter layer and minimal design impact. However, it has only marginal performance improvement and also the exposure light intensity is weakened. It means that the higher exposure dose, in other word, longer exposure time, is needed. Attenuated (halftone) PSM has the advantages of higher aerial image intensity and edge sharpness in the pattern transfer, but its total DOF is limited [1-9].

In this paper we report a new type of PSM, namely, halftone-rim, which is a combination of rim and halftone and has not been reported in literature so far. Rim, attenuated and halftone-rim PSMs are all suitable for the contact hole pattern transfer. The simulation, fabrication and contact hole pattern transfer of this halftone-rim PSM are studied.

2. EXPERIMENTAL

The positive tone e-beam resist on mask used is ZEP-520 with a thickness of 0.5 μm. The developer of this resist is xylene. E-beam exposure was carried out with a JEOL JBX 5D-II under spot size of 8 nm and 50 kV. E-beam exposure dose to resist is 35 $\mu C/cm^2$. The phase shifter layer is SiO_2 which has a refractive index of 1.44 and a thickness of ~4200Å. The dry etching of shifter layer was done by reactive ion etching (RIE) with following conditions: CF_4/O_2=95:5 sccm; 53 mTorr; 200W, 5~7 min. The wet etch of halftone chrome which has a intensity transmittance of 15 % was done by dip in HF/H_2O=1:25 for 5 min first then in CR-7 (ceric ammonium nitrate) for 1 min. Pattern transfer was performed by a Nikon NSR-I8 5X i-line stepper which has a NA of 0.5 and a coherence of 0.6. SEM were taken by a JEOL JSM 6300F. The positive tone photoresist on the 6" wafer is TOK IP-3100 with a thickness of 1.12 μm. The developer is TOK NND-W. Exposure time on the photoresist is 250 ms (exact exposure dose is not sure). The simulation tool is Depict-2 from Technology Modeling Associates, Inc. (TMA).

3. RESULTS AND DISCUSSION

Simulation studies with Depict-2 simulation tool indicate that halftone-rim is suited better for the making of contact hole, but not for line and space. Hence, this paper concentrated on the study of pattern transfer of 0.35 μm contact hole only. Fig. 1 indicates the structures of various masks including halftone-rim. Halftone-rim PSM has a self-aligned effect, therefore, fabrication processes become easier compared to subresolution PSM as shown in Fig 2.

 0-8194-1356-9/94/$6.00

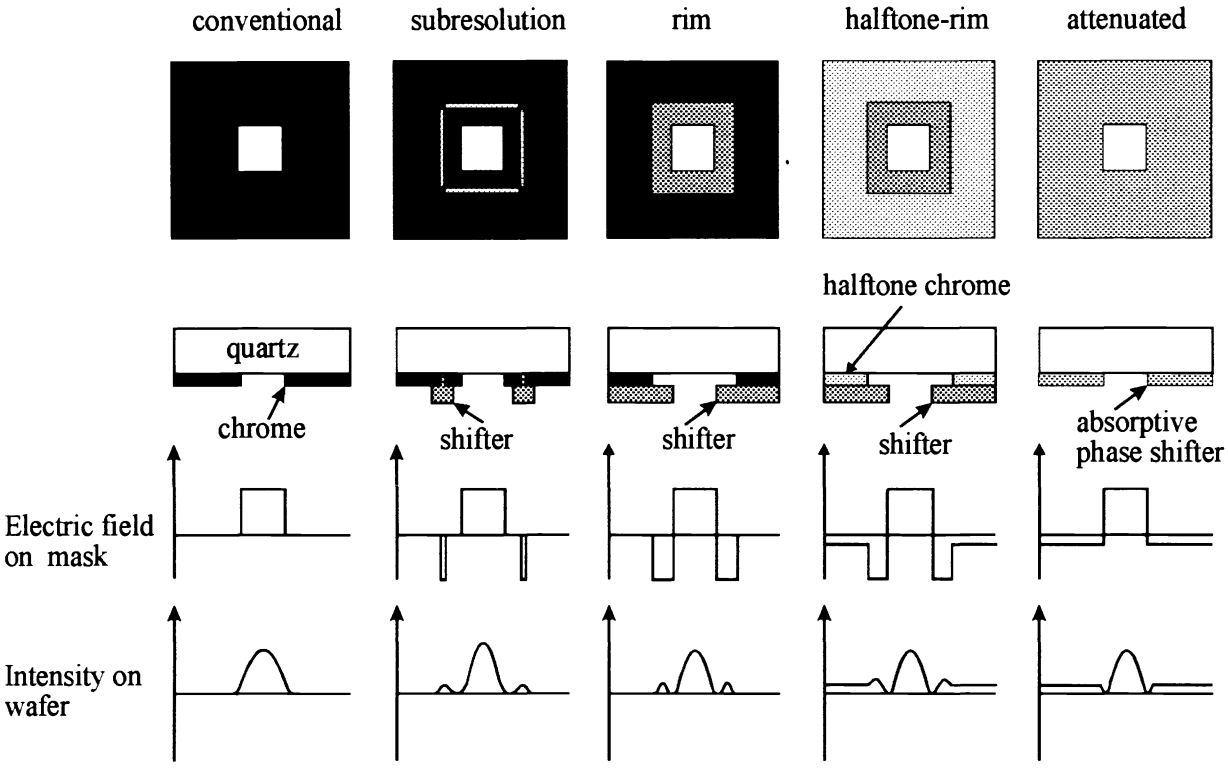

Fig. 1 Typical structures of conventional chrome mask and various phase shifting masks.

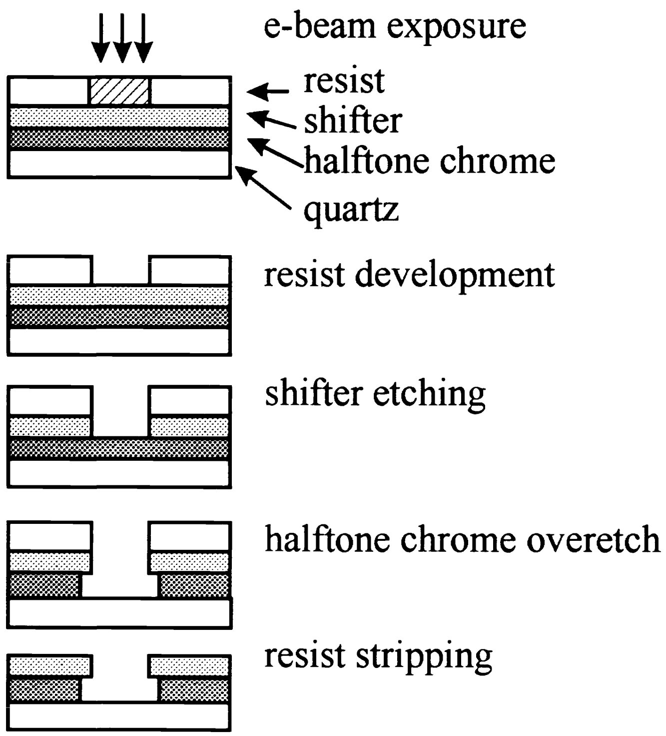

Fig. 2 Fabrication sequence of a halftone-rim phase shifting mask.

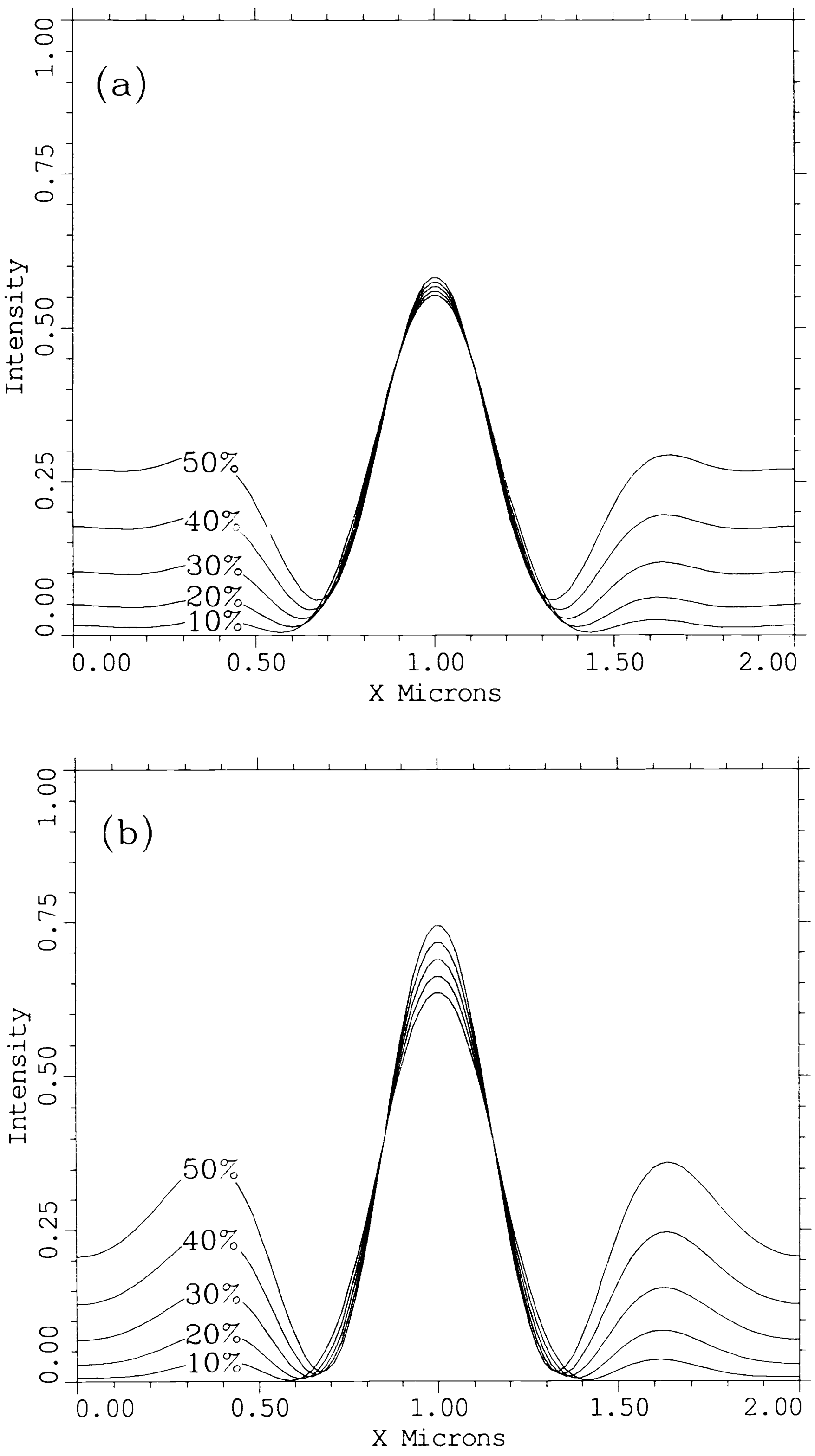

Fig. 3 Aerial images of halftone-rim PSM for 0.35 μm contact hole with various amplitude transmittance (mask edge: 2 μm; aperture width on shifter: 0.5 μm; rim width 0.05 μm; NA: 0.5; defocus: 0 μm). (a) coherence: 0.6; (b) coherence: 0.3.

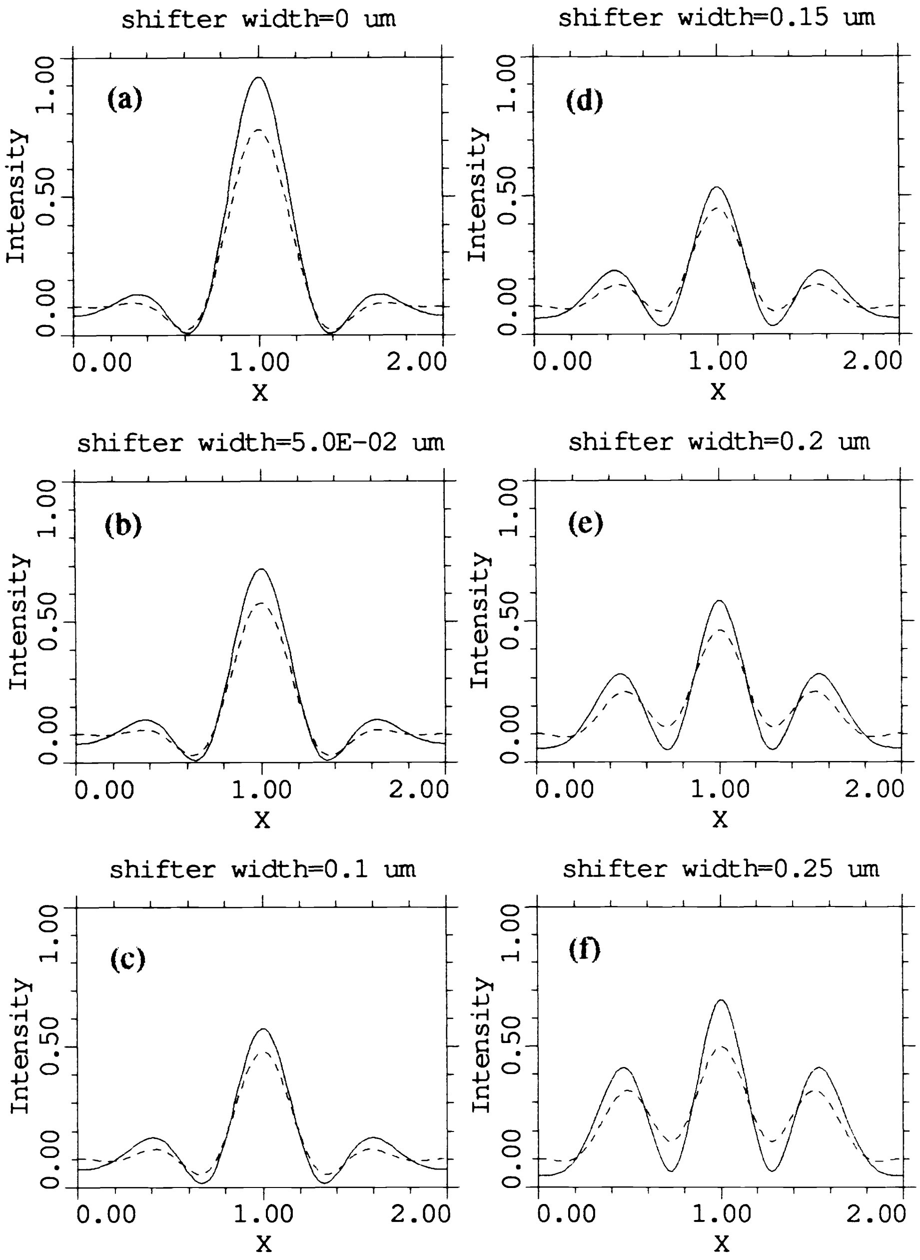

Fig. 4 Aerial images of halftone-rim PSM for 0.35 μm contact hole with various rim width (shifter width) at 30 % amplitude transmittance. Solid line: coherence 0.3. Dotted line: coherence 0.6.

Aerial images of halftone-rim PSM for 0.35 μm contact hole with various amplitude transmittance at different coherence are shown in Fig. 3. Obviously, lower coherence is favored for the PSM. The amplitude transmittance of halftone region up to 30 % (9 % for intensity transmittance) is acceptable for the photoresist exposure. The intensity transmittance of halftone region can not be too high in order to prevent the development of photoresist in the unexposed area.

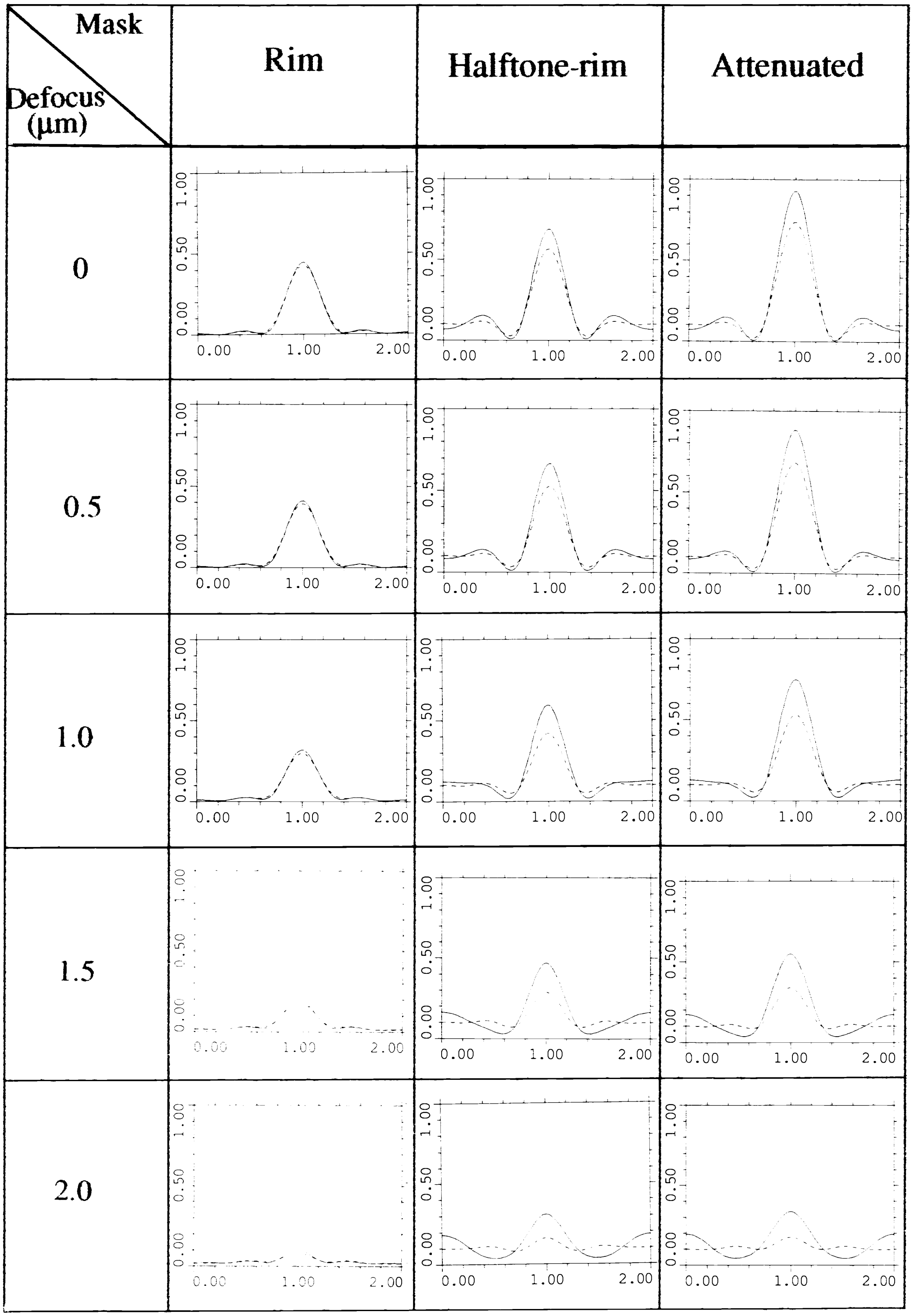

Fig. 5 Comparison of aerial images of rim (aperture width: 0.5 µm; rim width: 0.1 µm), halftone-rim (aperture width: 0.5 µm; rim width: 0.05 µm, amplitude transmittance: 30 %) and attenuated (aperture width: 0.5 µm, amplitude transmittance: 30 %) PSMs at various defocus distance. Solid line: coherence 0.3. Dotted line: coherence 0.6.

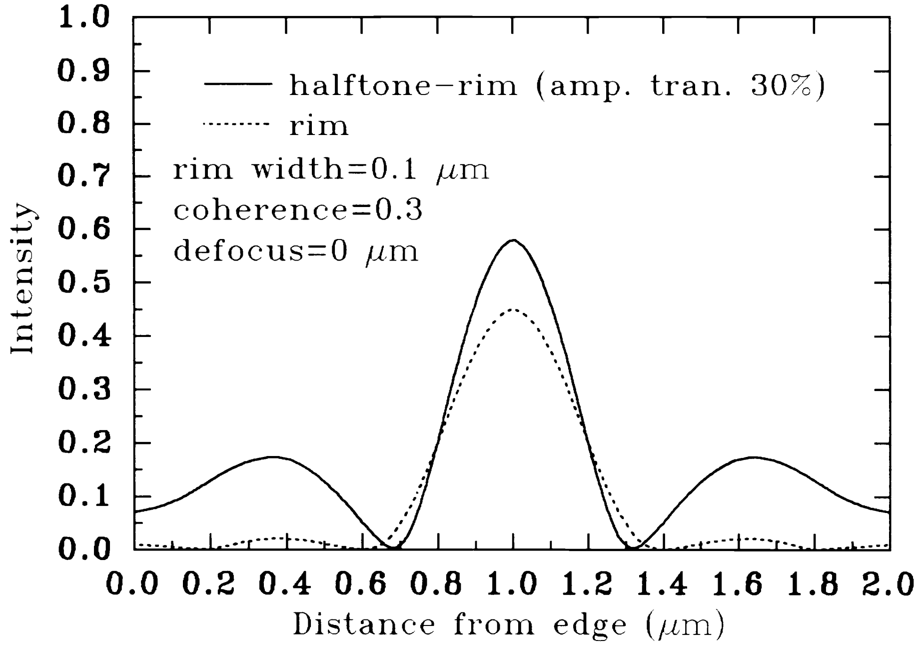

Fig. 6 Aerial images of rim and halftone-rim PSMs for 0.35 μm contact hole. The aperture is 0.50 μm for both masks.

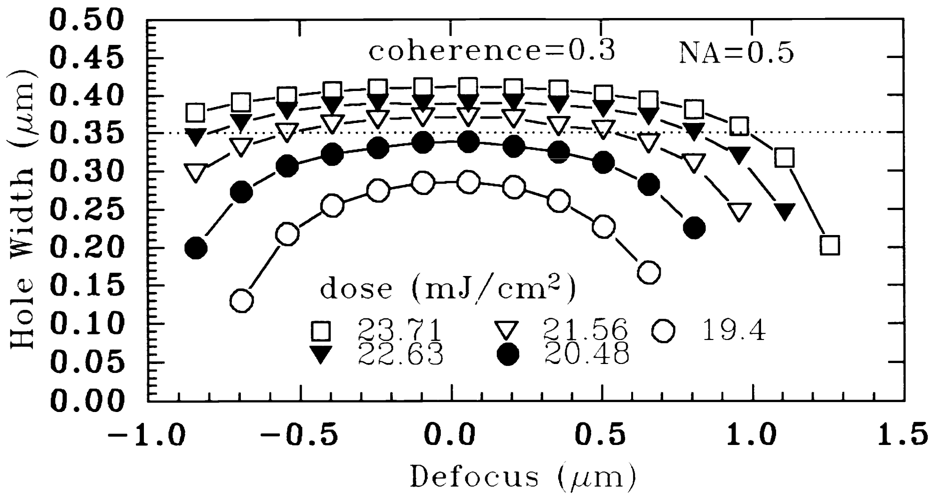

Fig. 7 Exposure-defocus matrix of halftone-rim PSM for 0.35 μm contact hole (aperture width: 0.5 μm; rim width: 0.05 μm; amplitude transmittance: 30 %).

Aerial images of halftone-rim PSM for 0.35 μm contact hole (aperture width on mask is 0.5 μm) with various rim width (shifter width) at 30 % amplitude transmittance is shown in Fig. 4. Rim width range of 0.05~0.1 μm (Fig. 4b & 4c) is a better choice since they have high enough intensity and narrower width of center maximum which is critical to the contact hole resolution. When amplitude transmittance is greater than 30 %, the intensity of first maximum (next to the center maximum) becomes to strong, and is no longer suitable to be a photomask as mentioned before.

Fig. 5 and Fig. 6 indicate the comparison of aerial images of rim, halftone-rim and attenuated PSMs at various defocus distance. Halftone-rim has the narrowest center maximum at the whole defocus range of testing. Although the attenuated PSM has higher intensity than halftone-rim, however, the intensity drops sharply as the defocus increasing when compared with halftone-rim and results in the shorter total DOF than halftone-rim.

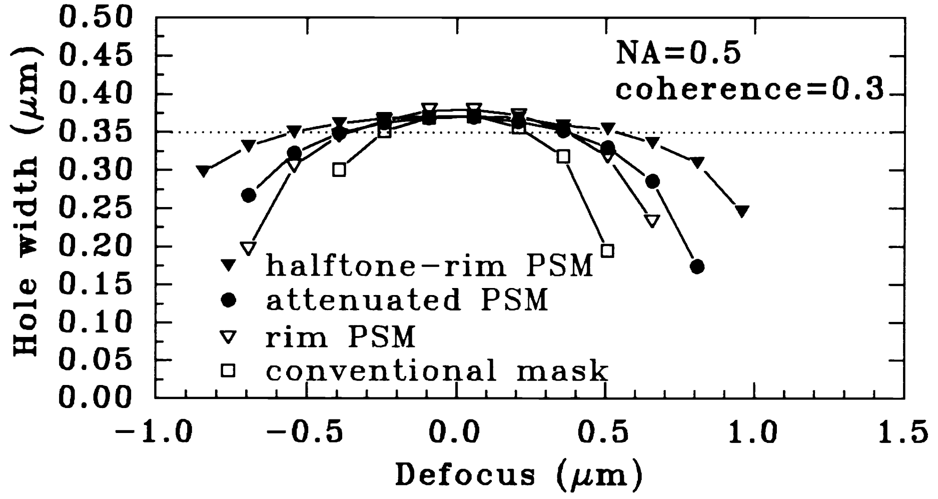

Fig. 8 The simulated contact hole width in photoresist vs. defocus using various masks at optimized conditions (The aperture of conventional chrome mask is 0.35 μm. The rest are same as in Fig. 5).

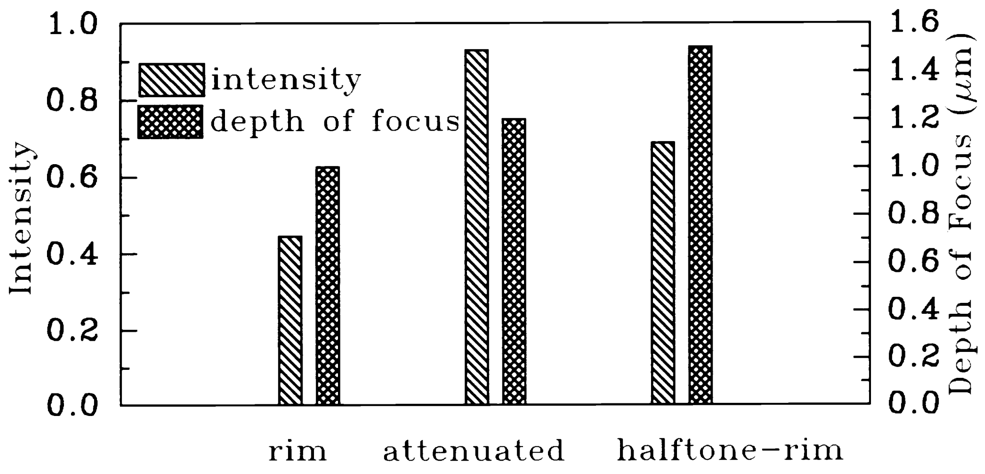

Fig. 9 The center maximum intensity of aerial image and total depth of focus of rim, halftone-rim and attenuated PSMs. The maximum C.D. variation allowed is 0.35 μm ±10 %.

Halftone-rim has a fair exposure latitude and a good defocus latitude as shown in Fig. 7. In Fig. 8, contact hole width using various masks is compared at their optimized conditions to designed size of 0.35 μm. Halftone-rim has the largest focus latitude among all these masks.

Fig. 9 illustrates that the halftone-rim has the largest total DOF among these three PSMs. It is worth to mention that attenuated PSM is same as the halftone-rim with a zero rim width. The shorter DOF of attenuated PSM is caused by the sharp intensity drop as the defocus increasing.

Simulated sidewall profiles of developed positive tone resist using halftone-rim PSM with various amplitude transmittance at optimized conditions are shown in Fig. 10. As mentioned earlier, 30% is maximum amplitude transmittance for practical application as indicated in Fig. 10 (c).

The Summaries of simulated results of various PSMs for 0.35 μm contact hole are shown in Table. 1.

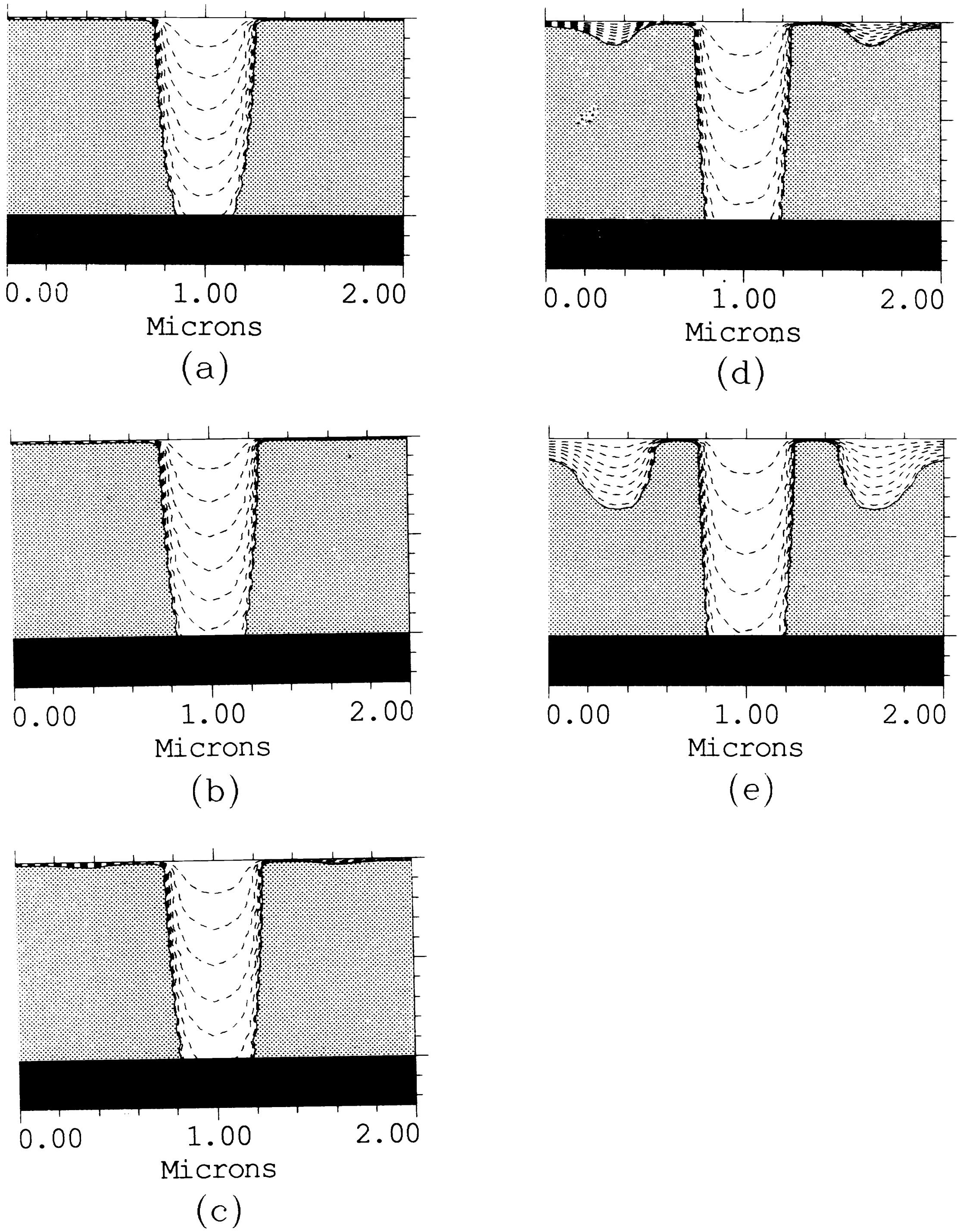

Fig. 10 Simulated sidewall profiles of halftone-rim PSM with various amplitude transmittance at optimized conditions as follows: mask edge: 2 μm; aperture width on shifter: 0.5 μm; rim width 0.05 μm; NA: 0.5; coherence: 0.3; defocus: 0 μm; resist thickness: 1 μm; Dill's parameter: A= 0.73 μm^{-1}; B= 0.08 μm^{-1}; C= 0.1 cm^2/mJ; Development parameter: U1=5; U2=0.03; U3=5; U4=0.24; U5= 0.55; U6= 0.65. Post exposure bake: 100°C, 45 sec. Development time: 45 sec.
Amplitude transmittance: (a) 10 %; (b) 20 %; (c) 30 %; (d) 40 %; (e) 50 %.

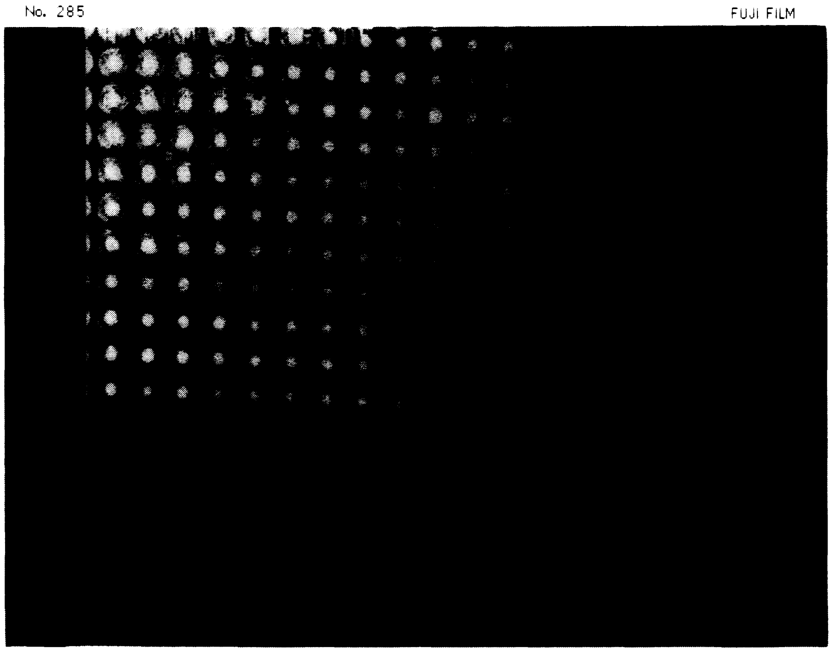

Fig. 11 Bird's-eye view of 0.35 μm contact hole patterns on the positive tone photoresist/wafer.

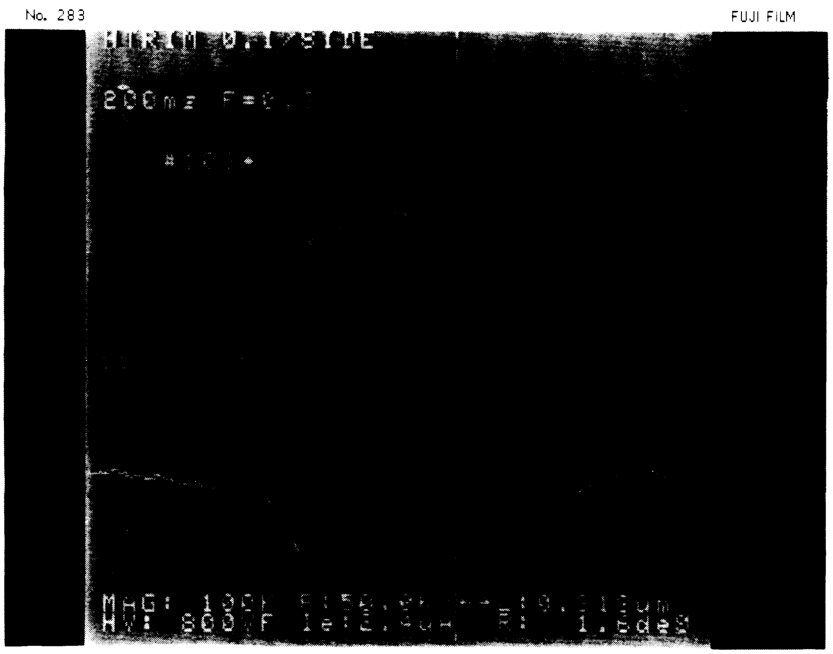

Fig. 12 Close-up view of 0.35 μm contact hole patterns on the positive tone photoresist/wafer.

Table 1. Summaries of simulated results of PSMs for 0.35 μm contact hole*.

	Rim	Halftone-rim	Attenuated
Resolution improved (defocus = 0~2 μm)	15~144%	18~160%	17~142%
Intensity improved (defocus = 0~2 μm)	37~110%	115~540%	190~620%
Total depth of focus (DOF) (μm)	1.0	1.5~1.6	1.2
Coherence (σ) required	moderate	low (0.3~0.35)	low (0.3~0.35)
Dose required (mJ/cm^2)	33.5	21.5	15.5
Positive mask bias (λ / NA)	0.34	0.27	0.20
Amplitude transmittance required (%)	-----	< 30 %	< 30 %
Intensity transmittance required (%)	-----	< 9 %	< 9 %

*Compared with 0.35 μm conventional chrome (Cr) mask at optimized conditions.

Bird's-eye view of contact hole patterns on the photoresist/wafer is shown in Fig. 11. Close-up view of contact hole patterns on the photoresist/wafer is shown in Fig. 12. The experimental check-up so far in our laboratory using this halftone-rim PSM could not reach the resolution and DOF from the simulation study. EDS study on the halftone-rim mask indicates the presence of a thin layer of chrome at the location of aperture center which is supposed to be free of chrome after the fabrication of mask. It is postulated that during the reactive ion etching (RIE) of shifter layer, a thin film is formed on top of chrome by sputtering coating, and preventing the wet etching of chrome layer and also resulting the seriously lateral etching (undercut) of halftone chrome layer. The intensity transmittance of halftone region of our halftone-rim mask is about 15 % which is much higher than 9 % of optimized transmittance. Defocus is found to be 0.3 ~ -0.6 μm in this check-up. Contact holes smaller than 0.31 μm could not be resolved by this halftone-rim mask so far. For the comparison purpose, contact holes smaller than ~0.45 μm could not be resolved by conventional chrome mask without phase shifting technique under same conditions.

4. CONCLUSION

The simulation studies indicate that halftone-rim PSM has a better resolution and larger total DOF for 0.35 μm contact hole compared with rim and attenuated PSMs. The experimental results of preliminary pattern transfer studies so far using this new type PSM could not reach the results of resolution and DOF from the simulation. The control of thickness of shifter; vertical sidewall profile of shifter by RIE; the wet etching of halftone chrome, therefore, the width of rim; the exposure dose for pattern transfer etc. are all critical to this study. Further experimental works on optimization of lithographic processes are needed to improve both resolution and total DOF. The applications of halftone-rim PSM for line and space pattern transfer did not show meaningful improvement compared with Levenson and shifter-only types by simulation studies, therefore, are not reported in this paper.

5. ACKNOWLEDGEMENT

This work was financially supported by the National Science Council and United Microelectronics Corp. (UMC) of R. O. C.

6. REFERENCES

1. M.D. Levenson, IEEE on Transactions on Electron Devices, ED-29, No.12, p.1828 (1982).
2. M.D. Levenson, SPIE, Vol. 1496, p. 20 (1990).
3. G. E. Flores and B. Kirkpatrick, IEEE Spectrum, October, p. 24 (1991).
4. B. J. Lin, BACUS News, Vol.7, Issue 1, Feb., 1991.
5. N. Samoto, Y. Makino, K. Onda, E. Mizuki and T. Itoh, J. Vac. Sci. Technol., B8(6), Nov/Dec, p. 1335 (1990).
6. S. K. Dunbrack, A. Muray, C. Sauer and R. L. Lozes, SPIE, Vol. 1464, p. 314 (1991).
7. K. Kamon and T. Miyamoto, Jan. J,. Appl. Phys., Vol. 31, No. 12B, Part 1, Dec., p. 4131 (1992).
8. B. J. Lin, Solid State Technology, Jan., p. 43 (1992).
9. Semiconductor International, July, p. 184 (1993).